Preparation of Porous Electro-Spun UPM Fibers via Photocrosslinking

Liu Jun, Yu Zhang, Yu Hao, Long Cheng, Zhang. J. J.

State Key Laboratory for Modification of Chemical Fibers and Polymer, Materials, College of Material Science and Engineering, Donghua University, Shanghai 200051, People's Republic of China

Received 25 February 2008; accepted 21 November 2008
DOI 10.1002/app.29778
Published online 13 February 2009 in Wiley InterScience (www.interscience.wiley.com).

ABSTRACT: In this study, a new method of preparing porous ultra-fine fibers via photocrosslinking was developed. Ultra-fine unsaturated polyester macromonomor (UPM)/poly(3-hydroxybutyrate-*co*-3-hydroxyvalerate) (UPM/PHBV) blend fibers were electrospun and then the UPM was photocrosslinked by UV irradiation. Different ratios between UPM, PHBV and solvent were tested and the relationship between weight percentage of solutions and diameter of fibers was discussed. Through the test of T_g and T_m we found that UPM and PHBV were immiscible and the phase separation proceeded during the electrospinning. The photocrosslinking time was controlled strictly and the best reaction time can't exceed more than 10 min. After photocrosslinking of UPM, PHBV was extracted from the blend fibers with chloroform. The morphology of the fiber was observed through SEM and fibers were not collapsed during the extracted processing. © 2009 Wiley Periodicals, Inc. J Appl Polym Sci 112: 2247–2254, 2009

Key words: porous fibers; electrospinning; unsaturated polyester macromonomor; poly(3-hydroxybutyrate-*co*-3-hydroxyvalerate); extract; photocrosslinking

INTRODUCTION

Electrospinning and the technologies of process have been paid much more attentions for building nanofibers. Polymer nanofibers with diameters are typically in the range from 100 to 10,000 nm[1] and their mats can show many distinctive properties such as high surface area-to-volume ratio, high porosity, and high absorption.[2] A lot of papers have reported many ways to modify nanofibers' properties. Normally people control the electrospinning condition such as solvent, solution properties, and additive type, to change the morphology of electrospun fibers.[3] Surface modification, heat treatment, and chemical crosslink was also used[4–6] to obtain fibers with thermal stability, solvent stability, and higher mechanical strength.

Porous ultra-fine fibers have much higher surface area-to-volume ratio and potential applications in filtration and drug carriers, etc.[29–30] Youk and coworker [7,8] studied porous ultra-fine fibers via selective thermal degradation and selective dissolution techniques, respectively. Although they got the porous structure yet lose the mechanical stability. Gupta et al.[9,10] prepared crosslinked porous ultra-fine fibers via photocrosslinking of poly(vinyl cinnamate)(PVCi) copolymers during electrospinning.[11,12] The irradiated PVCi copolymers formed an insoluble gel fraction due to intermolecular crosslink. After they washed the other blend polymer out, the porous and stability nano fibers were formed.

Photocrosslinkable polymers should have photoreactive groups or unsaturated groups in the main chain or side chain.[11–19] Unsaturated polyester macromonomor (UPM) is one of the unsaturated polyester (UP). UP have lots of good properties, such as good resistance against water, acids, oxidizing agents, organic solvents, light and weather. It is also one kind of nontoxic and environment-friendly material. Because of these merits, unsaturated polyester is wildly used in many different areas.[20–26]

UPM has two π-bond in the end group unit of main chain and can be excited during crosslinking reaction, as shown in Figure 1.

It is expected that photocrosslink porous ultra-fine fibers can be prepared via electrospinning of UPM with another immiscible polymer and subsequent removed the other polymer after photocrosslinking of UPM.

In our previous work, the preparation of a novel unsaturated polyester macromonomer (UPM) was

Correspondence to: Y. Zhang (yzh@dhu.edu.cn).
Contract grant sponsor: National Natural Science Foundation of China; contract grant number: 50803012.
Contract grant sponsor: Nano Special Project of Shanghai; contract grant number: 0352nm097.

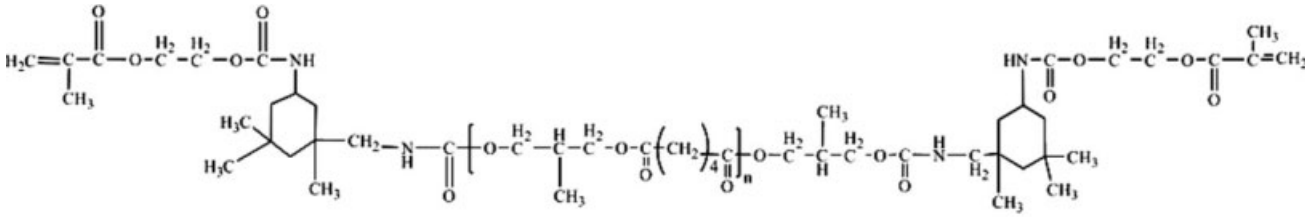

UPM

Figure 1 Chemical structures of UPM.

reported.[27] UPM could not be electrospun directly as result of its low viscosity, low molecular weight. So poly(3-hydroxybutyrate-*co*-3-hydroxyvalerate) (PHBV), another acyclic polyester, was used to improve the processability of the UPM.

In this article, we designed the wash process shown in Figure 2. for the preparation of porous ultra-fine fibers.

Ultra-fine UPM/PHBV fibers were firstly electrospun and then the PHBV was extracted with chloroform after the photocrosslinking of UPM. The acetone is a good solvent to the UPM monomer. So if the UPM is not crosslinked with other UPM monomer, it will be washed by acetone. And after fully crosslinked of UPM, we use chloroform to dissolve the PHBV. This method finally built the porous ultra-fine UPM fibers.

EXPERIMENTAL

Materials

UPM was prepared and reported in prework.,[27] chloroform and benzoyl peroxide (BPO) (initiator) were purchased from Sinopharm Chemical Reagent Co. Ltd. All the chemicals above are of analytical grade and used without further purification. Poly(3-hydroxybutyrate-*co*-3-hydroxyvalerate) (PHBV) (Mn 460,000, HV content 3%) were kindly supplied by Ningbo TianAn Co as an injection-molding grade and was purified before being used.

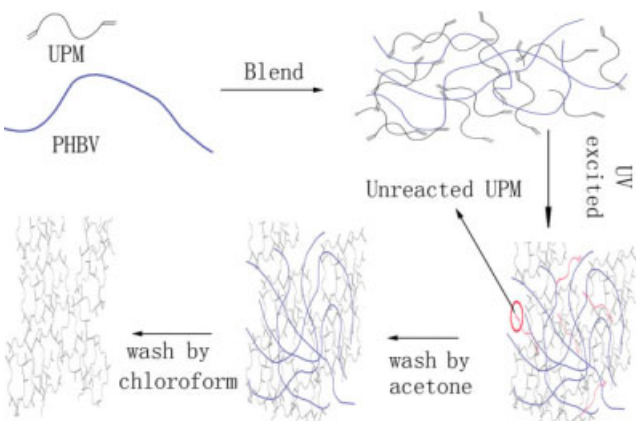

Figure 2 The process to implement the porous ultra-fine UPM fibers. [Color figure can be viewed in the online issue, which is available at www.interscience.wiley.com.]

Electrospinning

To prepare UPM/PHBV blend solutions, 10 wt % UPM and 10 wt % PHBV solutions in chloroform were prepared, respectively, and then they were mixed at predetermined ratios (UPM/PHBV = 4/1, w/w). Compared with solution, UPM/PHBV weight percentage was from 2.5 wt % to 25 wt % respectively, and final BPO was added as initiator. Initiator was not more than 1% compare with the weight ratio of UPM. The electrospinning setup used in this study consisted of a syringe and needle (9#), a ground electrode (d = 15 cm, stainless steel sheet on a drum), and a high voltage supply (Shanghai Shenfa Co, JG50-1) shown in Figure 4 top left. A syringe pump connected to the syringe controlled the flow rate. The electrospinning process was performed at a positive voltage of 14 kV, a working distance of 14 cm, and a mass flow rate was 0.8 mL/h.

Characterizations

For photocrosslinking, the electrospun UPM and UPM/PHBV mats were irradiated with UV light of wavelength 310–380 nm using a 1000 W high-pressure Hg lamp system (Self build). The thicknesses of these mats were in the range of 150–200 μm.

The photocrosslinking of UPM was analyzed by attenuated total reflection-Fourier transform infrared (ATR-FTIR) spectroscopy NEXUS-670, Nicolet in the mid-infrared range from 4000 to 500/cm. The morphologies and pore structures of electrospun UPM/PHBV and remaining UPM fibers were observed by a field emission scanning electron microscope (JSM-5600LV, JEOL) at 10 kV to 15 kV accelerating voltage. Prior to the observation, SEM specimens were

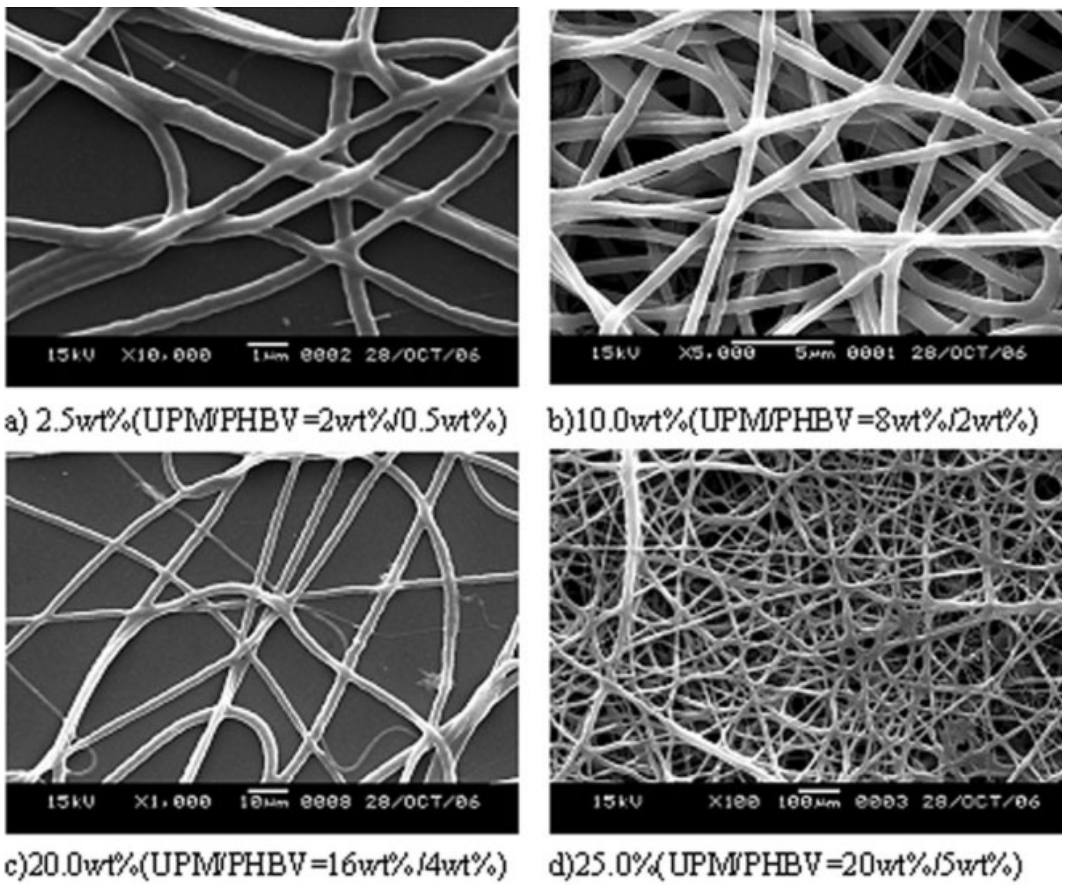

Figure 3 SEM micrographs of UPM/PHBV blend electrospun fibers after thermal crosslinking: (a) 2.5 wt %; (b) 10.0 wt %; (c) 20.0 wt %; (d) 25.0 wt %, the mass ratio of UPM to PHBV of all samples above is fixed to 4 : 1.

coated with platinum by ion beam sputtering for a few seconds. Thermal analysis was conducted on a Perkin-Elmer differential scanning calorimeter (Pyris-1) under a nitrogen atmosphere.

About 10 mg of sample was sealed in an aluminum pan for the measurement. To remove thermal history, the samples were heated to 200°C, held at this temperature for 1 min, and then quenched into liquid nitrogen. The samples were reheated from −40 to 200°C at a heating rate of 10°C/min.

RESULTS AND DISCUSSION

Jet radius and size distribution of UPM/Phbv ultra-fine fibers

In our prework we have discussed the UPM/PHBV blend electrospun fibers with different UPM/PHBV ratio, and the morphology of the fiber. Here, three different compositions of UPM, PHBV and BPO were electrospun.

Morphology of successfully electrospun UPM/PHBV fibers was shown in Figure 3. Submicron scale fibers were obtained for all the cases. We found that the all these fibers were roundshaped and the average diameters were 0.5 to 20 μm for ultra-fine UPM/PHBV(80/20) weight percentage from 2.5 wt % to 25 wt % respectively. The fibers' diameter increased significantly by increasing the weight percentage of UPM/PHBV. The results can be understood by the following argument. In the electrospinning, content of solute is a very important factor. The formation of the fine fibers is mainly achieved by the viscosity and acceleration of jets in high electric field.[23,28–33] Higher solute can result in a higher viscosity on the solution, thus the jet velocity was decreased and the same elongation forces cause the bigger diameter. Consequently, the diameter of the final fibers becomes gradually larger with the increase of solute. At same time, an increase in solute also enhanced the degree of instability of the jets in high solute field, which resulted in the more jumbled distribution of fiber diameters. As shown in Figure 3, the fiber distribution is becoming gradually broader with increasing the content of solute.

In this case the jet cross-sectional radius starting at the nozzle (at $z = 14$ cm) toward the grounded surface (at $z = 0$ cm) is observed. The onset point of the

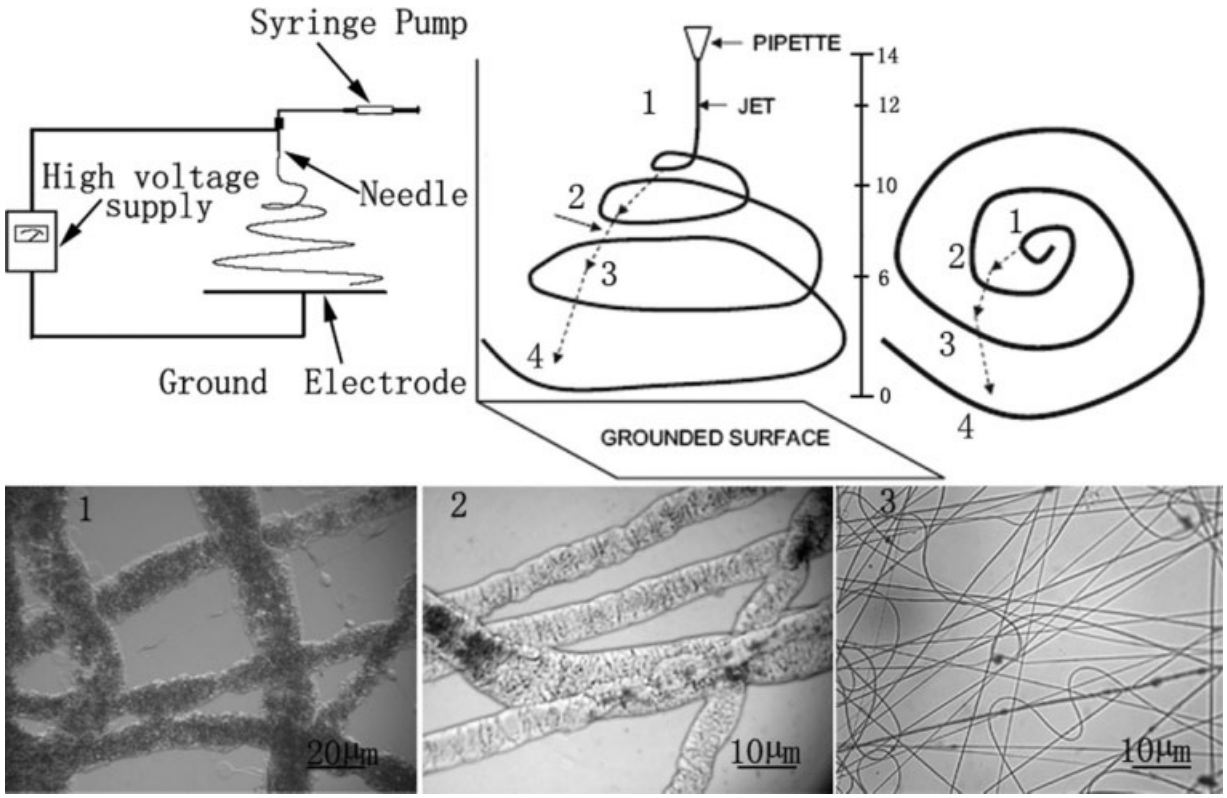

Figure 4 Top left: the figure of electrospinning setup; Top right: the 3D and top views of an instantaneous snapshot of an electrospinning; Base part: the optical microscope image of the jet in $z = 12$ cm, $z = 10$ cm, $z = 6$ cm, respectively.

bending instability (at $z = 10$ cm) and then the jet radius decreases very rapidly over a distance of only a few centimeters where fully developed bending instability appears (Fig. 4).

Figure 5 illustrates the effect of the initial polymer concentration on the jet radius, while all other parameter values are the same as for the base case. We find that at the beginning of the bending instability, the jet radius was very close. But with the fully developed bending loops the lower initial polymer concentration causes the smaller diameters.

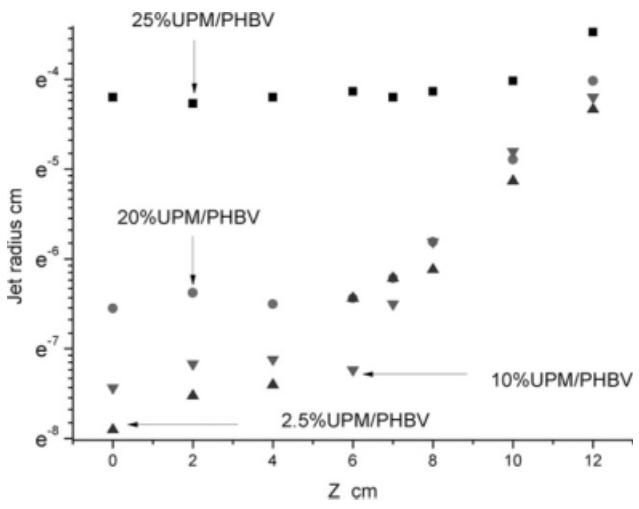

Figure 5 The cross-sectional radius of the jet measured from the nozzle below to grounded surface.

The decrease in jet cross-sectional radius is attributed to a strong repulsion of the fully developed bending loops below carrying electric charge of the same sign. And in the vigorously bending loops, the jet surface area increases dramatically as the jet undergoes huge stretching and elongation because of the electric forces. Such increase in the jet surface area dramatically accelerates solvent evaporation. The solvent concentration rapidly decreases in the bending loops, only a few centimeters below the onset of the bending instability (as seen in Fig. 4 from $z = 12$ to $z = 6$). Once the polymer concentration reaches about 90%,[34] the jet continues to elongate, but at a much lower rate, the radius of the jet loops changed slowly (as seen in Fig. 4 from $z = 6$ cm). The slower elongation rate is due to the increase in viscosity and elastic modulus of the solution at higher polymer concentrations. So the higher concentration UPM/PHBV firstly evaporation large part of the solvent and the radius also changed slowly. When the concentration of UPM/PHBV higher than 20% the fibers was not but the lower concentration UPM/PHBV still continue the process and get the smaller diameter fibers.

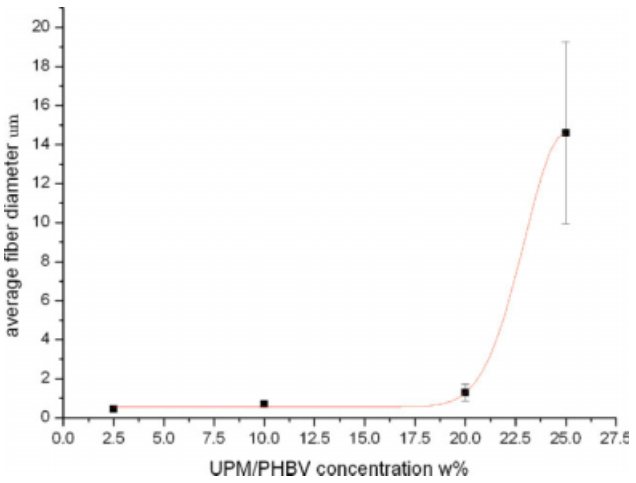

Figure 6 Relation between fiber diameter and UPM/PHBV concentration in the electrospinning at a constant applied voltage of 14 kV. [Color figure can be viewed in the online issue, which is available at www.interscience.wiley.com.]

And the relationship between average fiber diameter and fluctuation with polymer concentration is shown in Figure 6. It is reasonable to think that at a higher concentration the polymer tends to conglomerate so as to give a big fiber size.

Miscibility property of UPM/Phbv system

One of the most effective methods for determining the miscibility between polymer components is thermal measurement. When polymer components at the molecular level, single composition-dependent glass transition temperatures (T_g) between T_gs of the blend components is observed. If one of the blend components is crystallisable, its crystallization is hindered by a miscible pair, and so its melting temperature (T_m) and crystallinity are significantly decreased with the increasing content of the other component.[35–37] Table I present thermal properties of the UPM, UPM/PHBV blends, and PHBV. The distinctive glass transition temperatures (T_g) for PHBV in the ultra-fine UPM/PHBV fibers were clearly detected, however the glass transition temperatures (T_g) for UPM can not be tested even lower than −40°C. Moreover, the melting temperature (T_m) of PHBV was not significantly changed by various the blend ratio of ultra-fine UPM/PHBV blend fibers. Thus, UPM and PHBV are immiscible.

TABLE I
Thermal Properties of Electrospun UPM/PHBV Fibers

UPM/PHBV	T_g(°C)	T_m(°C)	ΔHm
100 : 0	—	23	52.3
75 : 25	−1.1	169	15.31
50 : 50	−1	171	23.43
25 : 75	−1.2	171	54.77
0 : 100	−1.2	169	62.11

UV crosslinking

The photocrosslinking of the ultra-fine UPM fibers was conducted to determine an appropriate irradiation time. Figure 7 shows collapse morphology by increasing photocrosslinking time. After irritation by UV more than 10 min, the fiber collapsed. It caused by UV decomposition.

As the UPM monomer is easy to resolved in acetone but the crosslinked structure is hard to resolve in acetone so for further crosslink ratio studies, 50 mg electrospun UPM/PHBV mat was cut. We irradiated it under UV beam from 0 to 30 min and then

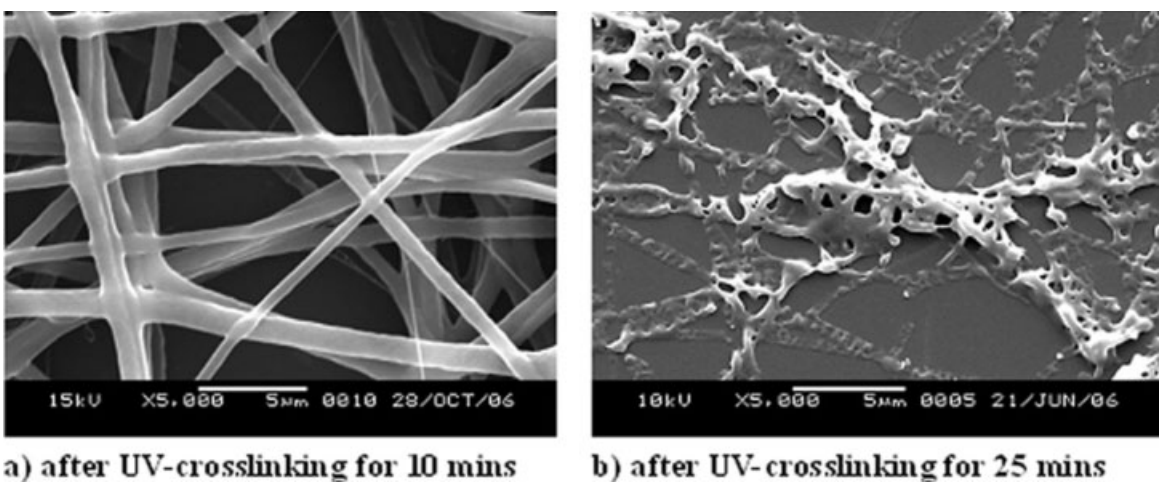

Figure 7 SEM micrographs of UPM/PHBV blend electrospun fibers after UV-crosslinking: (a) after UV-crosslinking for 10 mins, (b) after UV-crosslinking for 25 mins, all samples above were electrospun from solution with 10.0 wt %(UPM/PHBV = 4.0 wt % / 1.0 wt %).

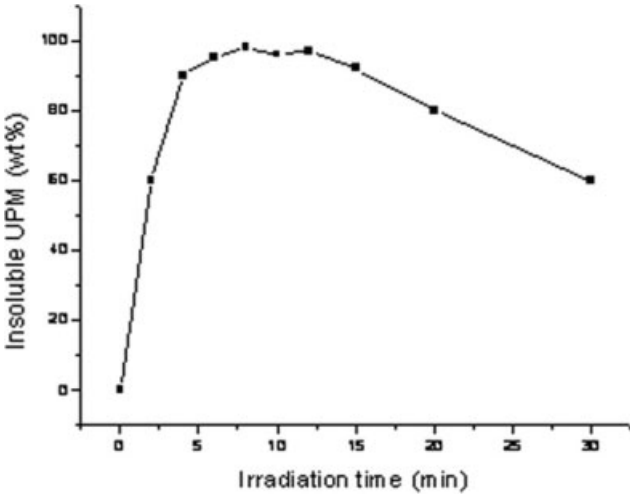

Figure 8 Insolubilization of UPM by photocrosslinking.

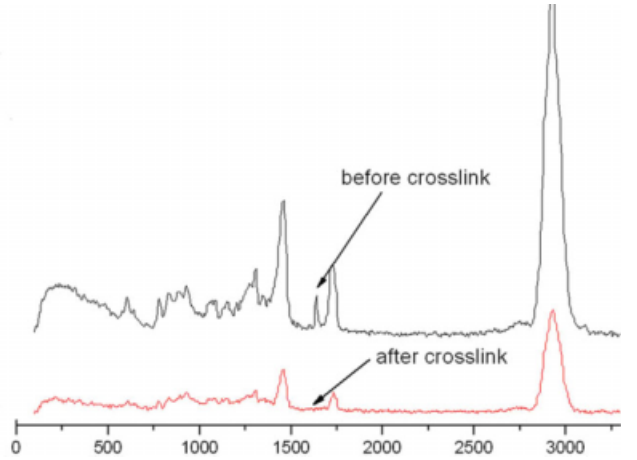

Figure 9 Raman spectra of UPM/PHBV blend electrospun fibers: (a) before photocrosslinking, (b) after photocrosslinking. [Color figure can be viewed in the online issue, which is available at www.interscience.wiley.com.]

mat was added to 10 mL acetone at 100 rpm at 90°C in a magnetic stirrer. After 30 min filtrating with the acetone, Mass loss (ML %) was evaluated by gravimetric analysis and calculated by:

$$\mathrm{ML}\% = 100(W_0 - W_t)/W_0 \quad (1)$$

where W_0 and W_t are the initial weight and the residual weight of the dry polymer at room temperature.[38–41]

Figure 8 shows the relationship between irradiation time and residual weight. From the figure, we can see that with the increasing of the irradiation time the residual weight increase gradually. After irradiation for more than 10 min the residual weight decreases quickly. It may caused by UV decomposition. Thus, the optimum irradiation period is 5 to 10 min. The residual weight is more than 95%. It can be explained that the high weight loss may be caused by insufficient UV irradiation or too long irradiation. If the π-bond didn't react fully, the crosslink can't build the network entirety. When the system was washed by acetone, unreacted UPM molecule solves in acetone. When the irradiation time is longer than 20 min, the irradiation acted too fury to make the action completely and the PHBV and UPM may decompose in bonds so that the fibers also lost their shape.

Figure 9 shows the Raman spectroscopy of UPM before and after photocrosslinking for 10 min. The major peaks for UPM at 1637 were attributed to C=C.[42] After UV irradiation for 10 min, the C=C stretching peak almost disappeared. The intensities of C=C vibrations were decreased according to the UV irradiation time. According to the results of Raman spectroscopy analysis and solubility test, in this study, the photocrosslinking of UPM in the ultra-fine UPM/PHBV blend fibers was conducted for 10 min.

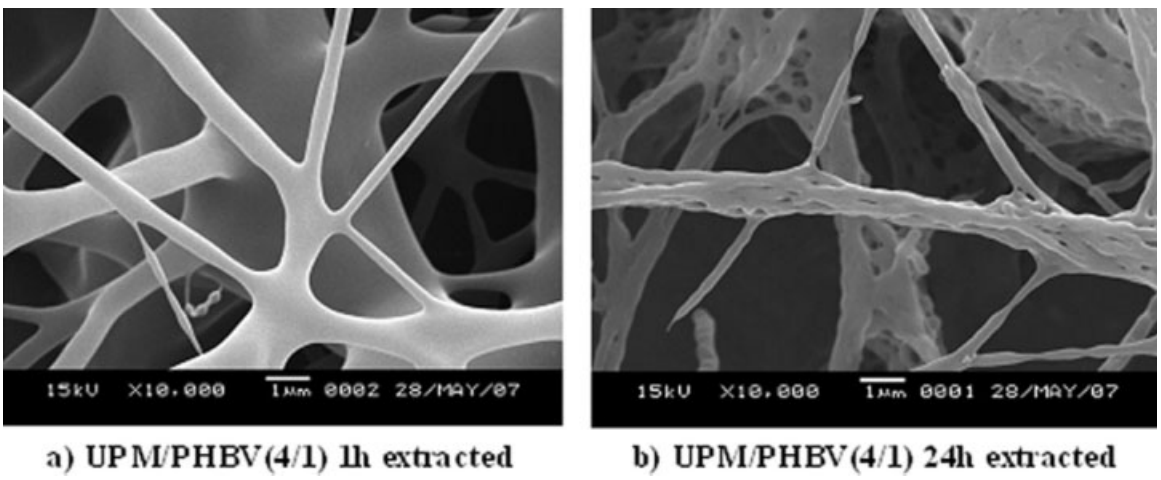

Figure 10 SEM images of UPM fibers remaining after PHBV extraction (a) UPM/PHBV (4/1) 1 h extracted (b) UPM/PHBV(4/1) 24 h extracted.

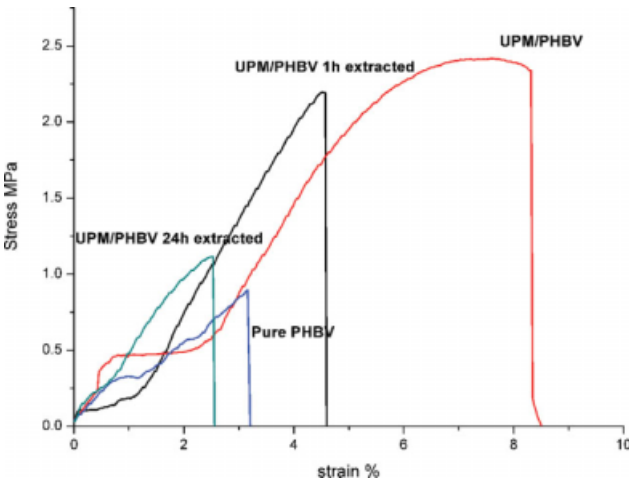

Figure 11 Stress–strain curves of PHBV; UPM/PHBV; extracted UPM/PHBV electrospun mat. [Color figure can be viewed in the online issue, which is available at www.interscience.wiley.com.]

The resulted porous fiber by extracting Phbv

Figure 10 shows the SEM images of UPM fibers remaining after PHBV extraction from photocrosslinked UPM/PHBV fibers. PHBV was extracted with chloroform from 1 h to 24 h. In the case of 1h extracted we found that the fiber structure was swelled and adhered together. With the increasing of extracted time we found that the fibers become the real porous fiber. From Figure 10, we can observe the different structure of the surface between 1 h extracting and 24 h extracting respectively. With 24 h washing, the weight of UPM remaining was very close to that of UPM in the original ultra-fine UPM/PHBV fibers.

It was reported that porous ultra-fine fibers can be electrospun by using highly volatile solvents for electrospinning.[43] The rapid evaporation of solvents during the electrospinning process resulted in the phase separation and then the polymer-rich phase forms the fiber matrix and the solvent-rich phase the pores. But as for UPM fiber, the structure is still kept as fibers, which may be caused by that the UPM, a crosslinked acyclic polyester oligomer. Because of the formation of the porous structure, we found that UPM and PHBV were phase separated on a scale smaller than the ultra-fine fiber diameter and the matrix dispersed morphology was also suggested by Bognitzki et al.[44,45]

The typical stress–strain curves of PHBV electrospinning mat, UPM/PHBV blends mat and the extracted mat are showed in Figure 11. For pure PHBV, its yield stress is 0.885 MPa, elongation at break is3.2%. But pure PHBV electrospun mat can't resist the extraction of chloroform and easiliy dissolved in the solution. As for crosslinked UPM/PHBV blends mat, the yield stress is 2.42 MPa while the elongation increases to 8.3%. It is found that with the increasing of extracted periods crosslinked mat still keep the mechanical property. Even it was extracted in chloroform for 24 h the mechanical properties is still higher than pure PHBV mat.

CONCLUSIONS

In this study UPM and PHBV were blended in 4 : 1. The ratio between solvent and solute were designed. The concentration of UPM/PHBV, distance from nozzle to collector in the electrospinning process were varied to determine their effect on final jet cross-sectional radius. The results show that such parameters have the large influence on the resulting electrospun fiber diameter. The average diameters of the ultra-fine UPM/PHBV fibers were in the range of 0.5–20 μm.

With the study of DSC, UPM and PHBV were immiscible and the phase separation proceeded during the electrospinning process.

The Raman spectra and residual weight of the polymer of UPM were detected before and after photocrosslinking. It is showed that the UPM's π-bond can be excited by UV light. The optimum photocrosslinking periods is 10 min.

After the photocrosslinking of UPM, PHBV was extracted from the UPM/PHBV blend fibers with chloroform. A porous structure was observed from the ultra-fine UPM fibers. In the cases of the ultra-fine UPM/PHBV(4/1) fibers, pores in the remaining UPM fibers can also prove the immiscible between PHBV and UPM.

The crosslinked electrospun fiber shows good solvent resistance property. The mat still keep mechanical property, even it was extracted in chloroform for 24 h.

References

1. Coleman, M. M.; Hu, Y.; Sobkowiak, M.; Painter, P. C. J Polym Sci Part B Polym Phys 1998, 36, 1579.
2. Suh, M. C.; Suh, S. C.; Shim, S. C.; Jeong, B. M. Synth Met 1998, 96, 195.
3. Rafferty, D. W.; Koenig, J. L.; Magyar, G.; West, J. L. Appl Spectrosc 2002, 56, 1549.
4. Chae, B.; Lee, S. W.; Ree, M.; Jung, Y. M.; Kim, S. B. Langmuir 2003, 19, 687.
5. Sung, S. J.; Cho, K. Y.; Yoo, J. H.; Kim, W. S.; Chang, H. S.; Cho, I. Park, J. K. Chem Phys Lett 2004, 394, 238.
6. Sung, S. J.; Cho, K. Y.; Park, J. K. Mater Sci Eng C Biomim Mater Sens Syst 2004, 24, 181.
7. Huang, Z. M.; Zhang, Y. Z.; Kotaki, M.; Ramakrishna, S. Compos Sci Technol 2003, 63, 2223.
8. You, Y.; Youk, J. H.; Lee, S. W.; Min, B. M.; Lee, S. J.; Park, W. H. Mater Lett 2006, 60, 757.
9. Gupta, P.; Trenor, S. R.; Long, T. E.; Wilkes, G. L. Macromolecules 2004, 37, 9211.
10. Chun, Y. S.; Kim, W. N. J Appl Polym Sci 2000, 77, 673.

11. Liu, W. J.; Yang, H. L.; Wang, Z.; Dong, L. S.; Liu, J. J. J Appl Polym Sci 2002, 86, 2145.
12. Maes, C.; Devaux, J.; Legras, R.; McGrail, P. T. Polymer 1995, 36, 3159.
13. Vaughan, A. S.; Stevens, G. C. Polymer 2001, 42, 8891.
14. Xiao, C.; Zhou, G. Polym Degrad Stab 2003, 81, 297.
15. Bognitzki, M.; Czado, W.; Frese, T.; Schaper, A.; Hellwig, M.; Steinhart, M.; Greiner, A.; Wendorff, J. H. Adv Mater 2001, 13, 70.
16. Bognitzki, M.; Frese, T.; Steinhart, M.; Greiner, A.; Wendorff, J. H. Polym Eng Sci 2001, 41, 982.
17. Lyoo, W. S.; Youk, J. H.; Lee, S. W.; Park, W. H.. Mater Lett 2005, 59, 3558.
18. Matthews, J. A.; Wnek, G. E.; Simpson, D. G.; Bowlin G. L. Biomacromolecules 2002, 3, 232.
19. Gibson, P.; Schreuder-Gibson, H.; Rivin, D. Colloid Surf A 2001, 187, 469.
20. Barbosa-Coutinho, E.; Salim, V. M. M.; Borges, C. P. Carbon 2003, 41, 1707.
21. You, Y.; Lee, S. W.; Lee, S. J.; Park, W. H. Mater Lett 2006, 60, 1331.
22. Ding, B.; Kim, H. Y.; Lee, S. C.; Shao, C. L.; Lee, D. R.; Park, S. J.; Kwag, G. B.; Choi, K. J. J Polym Sci Part B: Polym Phys 2002, 40, 1261.
23. Zeng, J.; Hou, H. Q.; Wendorff, J. H.; Greiner, A. Macromol Rapid Commun 2005, 26, 1557.
24. Li, L.; Hsieh, Y. L. Polymer 2005, 46, 5133.
25. Caruso, R. A.; Schattka, J. H.; Greiner, A. Adv Mater 2001, 13, 1577.
26. Hou, H.; Jun, Z.; Reuning, A.; Schaper, A.; Wendorff, J. H.; Greiner, A. Macromolecules 2002, 35, 2429.
27. Dai, T.-H.; Yu, H.; Zhang, K.; Zhu, M.-F. J Appl Polym Sci 2008, 107, 2142.
28. Yuan, H. Y.; Lu, X. Y.; Zeng, Z. H.; Yang, J. W.; Chen, Y. L. J Appl Polym Sci 2004, 92, 2765.
29. Prabu, A. A.; Alagar, M. Prog Org Coat 2004, 49, 236.
30. Kim, S. H.; Kim, S. H.; Nair, S.; Moore, E. Macromolecules 2005, 38, 3719.
31. Yi, F.; Guo, Z. X.; Hu, P.; Fang, Z. X.; Yu, J.; Li, Q. Macromol Rapid Commun 2004, 25, 1038.
32. Choi, S. S.; Hong, J. P.; Seo, Y. S.; Chung, S. M.; Nah, C. J Appl Polym Sci 2006, 101, 2333.
33. Buttafoco, L.; Kolkman, N. G.; Buijtenhuijs, P. E.; Poot, A. A.; Dijkstra, P. J.; Vermes, I.; Feijen, J. Biomaterials 2006, 27, 724.
34. Thompson, C. J.; Chase, G. G.; Yarin, A. L.; Renekerc, D. H. Polymer 2007, 48, 6913.
35. Smith, A. L. Ind Eng Chem 1954, 46, 1613.
36. Milkovich, R. Polym Prepr 1980, 21, 40.
37. Tie, S. H.; Qiu, K.Y. Acta Polym Sinica 1990, 8, 509.
38. Fang, S. M.; Zhou, L. M.; Zhang, L.C. Polym Mater Sci Eng (Chinese) 2004, 20, 109.
39. Semsarzadeh, M. A.; Navarchian, A. H. J Polym Eng 2003, 23, 225.
40. Burel, F.; Feldman, A.; Bunel, C. Polymer 2005, 46, 15.
41. Fernanda, M. B. C.; Delpech, M. C.; Alves, L. S. J Appl Polym Sci 2001, 80, 566.
42. Polus, I. Holz als Roh- und Werkstoff 2003, 61, 238.
43. Romanova, V.; Begishev, V.; Karmanov, V.; Kondyurin, A.; Maitz, M. F. J Raman Spectrosc 2002, 33, 769.
44. Bognitzki, M.; Hou, H.; Ishaque, M.; Frese, T.; Hellwig, M.; Schwarte, C.; Schaper, A.; Wendorff, J. H.; Greiner, A. Adv Mater 2000, 12, 637.
45. Lyoo, W. S.; Youk, J. H.; Lee, S. W.; Park, W. H. Mater Lett 2005, 59, 3558.